Journal Pre-proof

SVCT2-DEPENDENT PLASMA AND MITOCHONDRIAL MEMBRANE TRANSPORT OF ASCORBIC ACID IN DIFFERENTIATING MYOBLASTS

Mara Fiorani, Maddalena Scotti, Andrea Guidarelli, Sabrina Burattini, Elisabetta Falcieri, Orazio Cantoni

PII: S1043-6618(20)31350-5

DOI: https://doi.org/10.1016/j.phrs.2020.105042

Reference: YPHRS 105042

To appear in: *Pharmacological Research*

Received Date: 27 January 2020

Revised Date: 17 June 2020

Accepted Date: 17 June 2020

Please cite this article as: Fiorani M, Scotti M, Guidarelli A, Burattini S, Falcieri E, Cantoni O, SVCT2-DEPENDENT PLASMA AND MITOCHONDRIAL MEMBRANE TRANSPORT OF ASCORBIC ACID IN DIFFERENTIATING MYOBLASTS, *Pharmacological Research* (2020), doi: https://doi.org/10.1016/j.phrs.2020.105042

SVCT2-DEPENDENT PLASMA AND MITOCHONDRIAL MEMBRANE TRANSPORT OF ASCORBIC ACID IN DIFFERENTIATING MYOBLASTS

*Mara Fiorani, Maddalena Scotti, Andrea Guidarelli, Sabrina Burattini, Elisabetta Falcieri and Orazio Cantoni

Dipartimento di Scienze Biomolecolari, Università degli Studi di Urbino Carlo Bo, 61029 Urbino, ITALY

Author e-mail address

Mara Fiorani, mara.fiorani@uniurb.it

Maddalena Scotti, maddalena.scotti@virgilio.it

Andrea Guidarelli, andrea.guidarelli@uniurb.it

Sabrina Burattini, sabrina.burattini@uniurb.it

Elisabetta Falcieri, elisabetta.falcieri @uniurb.it

Orazio Cantoni, orazio.cantoni@uniurb.it

Short title: mitochondrial SVCT2 in C2C12 cells

***Corresponding author:** Dr. Mara Fiorani, Dipartimento di Scienze Biomolecolari, Sezione di Biochimica e Biotecnologie, Università degli Studi di Urbino Carlo Bo, Via Saffi, 2; 61029 Urbino (PU), Italy. Tel: +39-0722-305241; Fax: +39-0722-305470; e-mail: mara.fiorani@uniurb.it

Graphical abstract

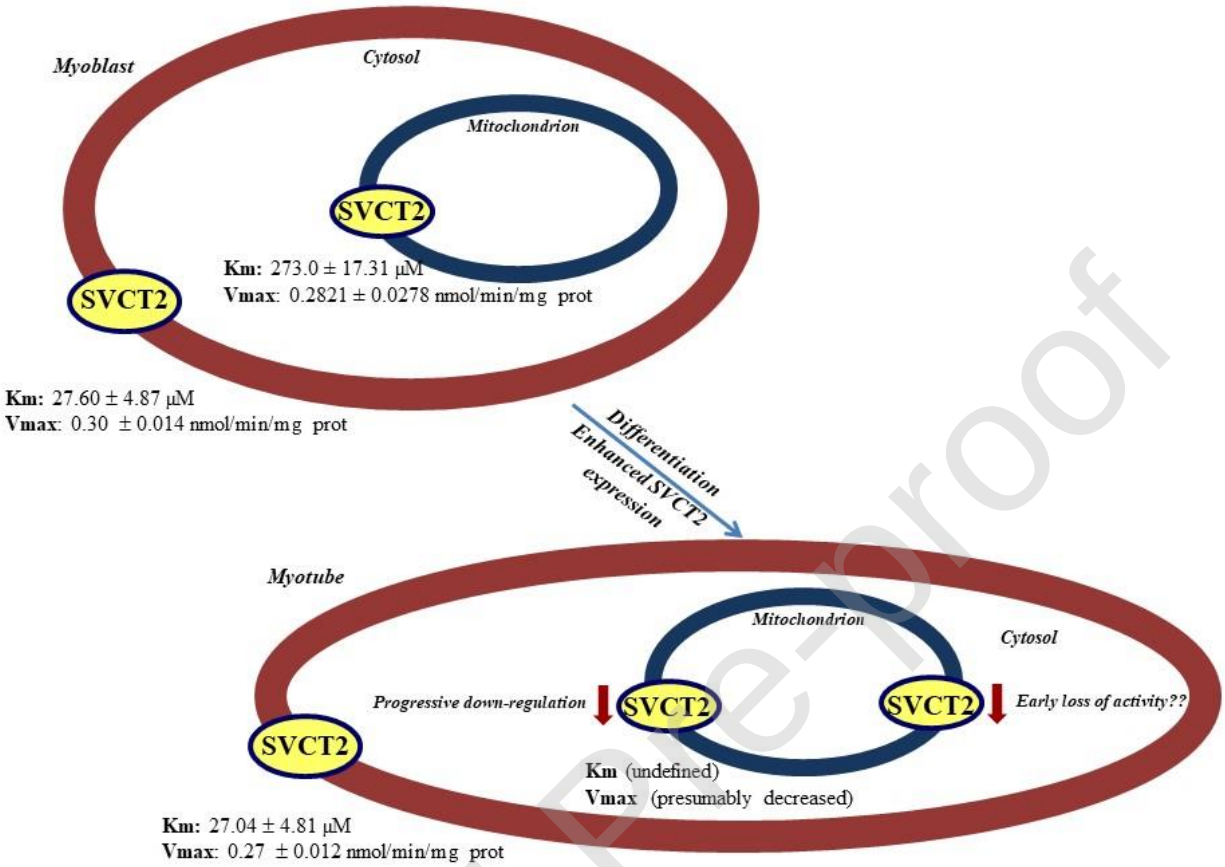

HIGHLIGHTS

- C2C12 myoblasts and myotubes express high affinity plasma membrane SVCT2.
- C2C12 myoblasts express low-affinity mitochondrial SVCT2.
- C2C12 myotubes present progressively reduced mitochondrial SVCT2 expression.

ABSTRACT

The Na^+-dependent Vitamin C transporter 2 (SVCT2) is expressed in the plasma and mitochondrial membranes of various cell types. This notion was also established in proliferating C2C12 myoblasts

(Mb), in which the transporter was characterised by a high and low affinity in the plasma and mitochondrial membranes, respectively. In addition, the mitochondrial expression of SVCT2 appeared particularly elevated and, consistently, a brief pre-exposure to low concentrations of Ascorbic Acid (AA) abolished mitochondrial superoxide formation selectively induced by the cocktail arsenite/ATP. Early myotubes (Mt) derived from these cells after 4 days of differentiation presented evidence of slightly increased SVCT2 expression, and were characterised by kinetic parameters for plasma membrane transport of AA in line with those detected in Mb. Confocal microscopy studies indicated that the mitochondrial expression of SVCT2 is well preserved in Mt with one or two nuclei, but progressively reduced in Mt with three or more nuclei. Cellular and mitochondrial expression of SVCT2 was found reduced in day 7 Mt. While the uptake studies were compromised by the poor purity of the mitochondrial preparations obtained from day 4 Mt, we nevertheless obtained evidence of poor transport of the vitamin using the same functional studies successfully employed with Mb. Indeed, even greater concentrations of/longer pre-exposure to AA failed to induce scavenging of mitochondrial superoxide in Mt. These results are therefore indicative of a severely reduced mitochondrial uptake of the vitamin in early Mt, attributable to decreased expression as well as impaired activity of mitochondrial SVCT2.

Abbreviations: AA, L-ascorbic acid; BSA, bovin serum albumin; CK, creatine kinase; DHA, dehydroascorbic acid; DTT, dithiothreitol; EB, extracellular buffer; ER, endoplasmic reticulum; GAPDH, glyceraldehyde 3-phosphate dehydrogenase; IB, intracellular buffer; IP_3R, inositol-1,4,5-trisphosphate receptor; HB, homogenizing buffer; FBS, fetal bovin serum, Mc, crude mitochondria; Mb, myoblasts; Mp, pure mitochondria; Mt, myotubes; MRB, mitochondria resuspending buffer; PBS, phosphate buffered solution; PM, plasma membrane; PVDF, polyvinyldiene difluoride membranes; ROS, reactive oxygen species; RT-PCR, reverse transcription-polymerase chain reaction; SVCT, sodium dependent vitamin C transporter; TEM, transmission electron microscopy.

Keywords: L-ascorbic acid; plasma membrane SVCT2; mitochondrial SVCT2; myoblasts; myotubes; C2C12 cells.

1. INTRODUCTION

L-ascorbic acid (AA) is a potent water-soluble antioxidant that scavenges reactive oxygen species (ROS) and mitigates oxidative stress *in vitro* and *in vivo* [1-3]. Its cellular accumulation is directly mediated by high affinity/low capacity Na^+-dependent transporters 1 and 2 (SVCT1 and 2) [4, 5], or indirectly, by hexose transporter-dependent transport of dehydroascorbic acid (DHA), the oxidised form of the vitamin, an event followed by prompt reduction back to AA [6, 7].

AA reaches significant concentrations in the cytosol as well as in specific subcellular compartments provided of adequate transport systems [8-10]. Mitochondria are sites of extensive ROS production, and are therefore equipped of an efficient antioxidant defence system, which includes AA [11]. Indeed, the vitamin may exert beneficial effects *via* direct ROS scavenging [12] and/or other effects related to vitamin E recycling [13]. Not surprisingly, significant levels of AA can be detected in mitochondria from different tissues *in vivo* [14-18].

For many years the possibility of an active transport of AA in mitochondria has not been considered likely, since the intracellular concentrations of the vitamin are in general very high and, most importantly, the cation (in particular Na^+ and Ca^{2+}) concentrations are dramatically lower than those required to support AA transport activity in the plasma membrane [5]. Hence, the prevalent idea was that DHA transport represents the main strategy for vitamin C accumulation in mitochondria, in particular under oxidative conditions in which mitochondrial ROS cause oxidation of the cytosolic fraction of AA in peri-mitochondrial regions, thereby transiently increasing the local concentrations of DHA [8, 19, 20].

We were therefore surprised to observe the mitochondrial expression of SVTC2 in U937 cell

mitochondria, in particular since this transporter was functional and characterised by a high affinity, with requirements for Na^+ and Ca^{2+} compatible with the cytosolic concentrations of these cations [21]. In another study, Munoz-Montesino et al. [22] also provided evidence for the mitochondrial expression of functional SVCT2 in cultured HEK-293T cells, however characterised by a low affinity. A common finding emerging from these studies, however, was that SVCT2 is remarkably more expressed in mitochondrial than in plasma membranes. More recently, this observation was confirmed in HEK-293T and HepG2 cells with the use of a novel fluorescent probe detecting SVCT2 [23]. A significant expression of SVCT2 was also found in the mitochondria of breast cancer cells, with hardly any expression detected in the mitochondria of normal breast tissue [24]. In addition, tumour cells failed to take up the vitamin *via* the same transporter, but rather used hexose transporters to accumulate large amounts of the vitamin in the form of DHA [24]. Prompt reduction of DHA to AA was then associated with the SVCT2-dependent transport of the vitamin in mitochondria.

It therefore appears that SVCT2 is expressed and functionally active in the mitochondria of various types of cells, an observation suggesting the physiological relevance of this transport mechanism of the vitamin, which nevertheless remains to be investigated in different cell types and tissues.

We thought that an interesting tissue is represented by the skeletal muscle which, while containing on a per cell basis less vitamin C than other cells in different tissues, nevertheless contains the largest fraction (about 65%) of the total body vitamin C [25-27], with approximately 3–4 mg AA per 100 g of tissue [25, 26, 28]. In addition, skeletal muscle cells are sites of extensive ROS production [29] and intramuscular AA contributes, in concert with other antioxidants, to the defensive machinery of these cells especially during intense physical activity [30], and in subjects with insulin resistance [31].

In order to learn more on mitochondrial SVCT2 expression and function in skeletal muscle cells, we decided to use a versatile murine cell line, C2C12 cells, widely employed to investigate events associated with the differentiation of myoblasts (Mb) to myotubes (Mt) [32, 33]. More specifically,

we investigated SVCT2 expression and activity in the plasma e mitochondrial membranes during the early phase of differentiation of Mb to Mt, a time at which the overall expression of the transporter was previously shown to increase [34]. We herein provide evidence for: i) increased SVCT2 expression during differentiation of Mb to early Mt, however associated with similar high affinity transport of AA in the plasma membrane; ii) elevated mitochondrial expression of SVCT2 and low affinity transport of AA in Mb; iii) rapid accumulation of AA in Mb mitochondria resulting in efficient scavenging of mitochondrial superoxide; iv) expression of SVCT2 maintained in early Mt, but nevertheless negatively modulated by the differentiation process, likely also in terms of activity of the residual SVCT2.

2. MATERIALS AND METHODS

2.1 Chemicals

AA, dithiothreitol (DTT), choline-chloride, sulfinpyrazone (S-pyr), 4-hydroxymercuribenzoic acid, (PCMB), sodium arsenite and ATP and most of the reagent-grade chemicals were purchased from Sigma-Aldrich (Milan, Italy). The antibodies against SVCT2 (sc-9926), cytochrome c (sc-7159) calnexin (sc-6465), HSP-60 (sc-13115), as well as the horseradish peroxidase-conjugated secondary antibodies (sc-2350; sc-2005) were purchased from Santa Cruz Biotechnology (Santa Cruz, CA); antibody against GLUT3 (ab53095) was from Abcam (Cambridge, UK). Ru360, Rhod 2-acetoxymethyl ester (AM), and MitoSOX red were purchased from Thermo Fisher Scientific (Milan, Italy).

2.2 Cell culture and treatment conditions

The mouse myoblast cell line C2C12 (ECACC 91031101, lot 12F005) was purchased from the European Collection of Authenticated Cell Cultures (ECACC, Salisbury, UK) and cultured in high-glucose D-MEM (Sigma-Aldrich) supplemented with 10% heat inactivated fetal bovine serum (FBS), 2 mM L-glutamine, 100 units/ml penicillin and 100 µg/ml streptomycin (Euroclone, Milan, Italy) in

a humidified atmosphere of 5% CO_2 at 37 °C. Cells at 60-70 % confluence were split 1:4 or 1:5. Upon 80-90% confluence, C2C12 myoblasts were stimulated to differentiate by changing the growth medium with D-MEM containing 1% heat inactivated FBS. Fresh D-MEM (1% heat inactivated FBS) was replaced daily. In all experiments reported in the present paper, C2C12 cells were used up to passage number 18.

Sodium arsenite was prepared as a 1 mM stock solution in saline A (140 mM NaCl, 5 mM KCl, 4 mM $NaHCO_3$, and 5 mM glucose, pH 7.4) and stored at 4 °C. Cells were exposed to arsenite, and/or other addictions, in D-MEM containing 1% heat inactivated FBS, as detailed in the text, as well as in the legends to the figures.

2.3 Purification of mitochondria and subcellular fractionation

C2C12 cells were processed to obtain the following sub-cellular fractions: crude mitochondria (Mc), pure mitochondria (Mp), plasma membrane (PM), endoplasmic reticulum (ER). Details on the fractionation protocols are given in refs [35, 36]. Briefly, the cells were washed twice in Phosphate Buffered Solution (PBS, 136 mM NaCl, 10 mM Na_2HPO_4, 1.5 mM KH_2PO_4, 3 mM KCl; pH 7.4) and detached with pre-warmed trypsin/EDTA solution (2.5 g/l trypsin plus 0.2 g/l EDTA). The cells were then transferred to a centrifuge tube, washed with PBS and re-suspended in ice-cold homogenization buffer (HB, 225 mM mannitol, 75 mM sucrose, 0.1 mM EGTA, protease inhibitor cocktail, 5 mM Tris-HCl, pH 7.4). The cells were homogenized with 30-40 strokes, by using a glass potter placed in an ice-bath. The efficiency of the homogenization process was monitored under the microscope by counting the number of residual trypan blue negative cells. The homogenate was centrifuged at 1000 *g* for 10 min at 4 °C and the supernatant (S1) collected for the final centrifugation. The pellet was re-homogenized and the supernatant (S2) added to S1 and centrifuged at 12000 *g* for 30 min at 4 °C. The pellet, corresponding to the Mc fraction was washed with HB, whereas the supernatant was centrifuged at 20000 *g* for 30 min at 4 °C to obtain the PM fraction. The final

supernantant was centrifuged at 95000 *g* for 90 min to obtain the ER fraction (pellet) and the cytosol (supernatant).

In order to obtain the Mp, the Mc fraction was gently re-suspended in the mitochondrial re-suspending buffer (MRB, 5mM HEPES, 250 mM mannitol, 0.5 mM EGTA, pH7.4) and centrifuged at 95000 *g* (4 °C) for 90 min on a 30% Percoll gradient. The lower density band, corresponding to the Mp fraction, was collected and washed two times with MRB [36].

2.4 Exposure of C2C12 cells and mitochondria to ascorbic acid.

C2C12 cells or isolated mitochondria were exposed for 10 min to AA in the presence of 0.1 mM DTT in extracellular buffer (EB, 15 mM Hepes, 135 mM NaCl, 5 mM KCl, 1.8 mM $CaCl_2$, 1 mM $MgCl_2$, pH 7.4) or intracellular buffer (IB, 15 mM Hepes-Na, 15 mM NaCl, 120 mM KCl, 1 mM $MgCl_2$, pH 7.6) respectively, and processed as described below. A 10 mM AA stock solution in EB or IB was prepared immediately before use. Stability of AA in EB or IB was assessed by monitoring the absorbance at 267 nm for 90 min (ε_{267} = 14,600 M^{-1} cm^{-1}). In selected experiments, NaCl of EB, or IB, was replaced with choline-chloride; in other experiments, HEPES-Na^+ and NaCl were replaced with choline-chloride in Na^+-free HEPES.

2.5 Transmission Electron Microscopy (TEM) analysis.

Cells were fixed with 2.5% glutaraldehyde in 0.1 M phosphate buffer (pH 7.4) for 15 min. Pellets were further processed as reported by Burattini et al. [37].

2.6 Immunolocalization by confocal microscopy

C2C12 cells were incubated for 20 min with 50 nM MitoTraker Red CMXRos (Molecular Probes, Europe, Leiden, The Netherlands) in 2 ml of PBS in 35-mm tissue culture dishes containing an uncoated coverslip. The cells were then fixed for 1 min with 4% paraformaldehyde, washed with PBS, permeabilized for 15 min with 0.1% Triton X-100 in PBS and then blocked for 30 min in PBS

containing bovine serum albumin (BSA, 2% w/v) at room temperature. The cells were subsequently incubated with goat polyclonal anti-SVCT2 antibody (1:100 in PBS containing 2% BSA), stored for 18 h at 4°C, washed and then exposed to FITC-conjugated secondary antibody diluted 1/100 in PBS for 2 h in the dark. The digital images were acquired on a Leica TCS-SP5 CSLM mounted on a Leica DMI 6000 CS inverted microscope (Leica Microsystems CMS GmbH, Mannheim, Germany) at 512 x 512 using 63.0 x 1.4 oil objective (HCX PL APO 63.0 x 1.40 OIL UV) and with appropriate excitation/detection settings (FITC argon laser 488 nm / 500-535 nm emission filter; MitoTracker Red HeNe laser 543 nm / 555-610 nm emission filter).

Images and degree of co-localization were analysed by the Leica Application Suite Advanced Fluorescence (LASAF) and JACoP, a plugin for the ImageJ Software (Wayne Rasband, Bethesda, MA). Pearson's coefficient was used to measure co-localization of SVCT2 with the mitochondrial probe.

2.7 Western blot assay

Equal amounts (30 µg) of sub-cellular fractions and whole cell lysates were resolved in 12.5 or 15% sodium dodecyl sulphate polyacrylamide gel and electro-transferred to polyvinyldiene difluoride membranes (PVDF). Western blot analyses were performed using antibodies against actin, SVCT2, cytochrome c, Hsp-60, calnexin and GLUT3. Details on the Western blotting apparatus and conditions are reported elsewhere [38].

2.8 Measurement of ascorbic acid content by HPLC

After treatments, the cells or mitochondria were washed twice with cold EB, or IB, respectively, and the final pellets were extracted with ice cold 70% (v/v) methanol/30% HPLC solution A (10 mM tetrabutylammonium hydrogen sulphate, 10 mM KH_2PO_4, 0.5% methanol, pH 6.0) containing 1 mM EDTA and 10 mM DTT. After a 10 min incubation at ice bath temperature, the samples were centrifuged at 10000 *g* for 20 min at 4 °C. Samples were filtered through a 0.22 µm filter (Millipore

Corporation, Billerica, MA, USA) and either analysed immediately or frozen at −80 °C for later analysis. AA content was measured by HPLC with the UV detection wavelength set at 265 nm, as described in [39], with minor modifications. The HPLC separation was performed using a 15 cm x 4.6 mm, 5 µm Supelco Discovery® C18 column equipped with a 5 µm Supelguard Discovery® 18 (2 cm x 4.0 mm) (Supelco, Bellefonte, PA, USA). The injection volume was 20 µl. Under these conditions the retention time of AA was about 4 min. AA concentration was determined from the corresponding calibration curve constructed with the pure chemical AA dissolved in the extraction solution.

2.9 Kinetic calculations

The transport kinetic parameters were calculated by using the Michaelis–Menten equation and the linear transformation of Eadie–Hofstee. Kinetic parameters were estimated from the fitted curves using the Graph Pad Prism software designed for nonlinear regression analysis.

2.10 Creatine kinase (CK) assay

Cells were washed twice in cold PBS and lysed in lysis buffer (3 mM phosphate buffer, pH 7.4; 5 mM glucose; 3 mM KF; 3 mM MSH; 1 mM DTT; 0.5 % Triton X-100). Lysates were then centrifuged at 10000 *g* for 10 min, and CK activity was measured in the supernatant. CK activity was determined spectrophotometrically at 340 nm, in a coupled enzyme system utilizing hexokinase and glucose 6-P dehydrogenase, as described in [40], with minor modifications. Specific CK activity was calculated after correction for total protein, determined by the Bradford method [41].

2.11 Reverse Transcription-Polymerase Chain Reaction (RT-PCR)

Total RNA was extracted with Trizol reagent (Invitrogen, Carlsbad, CA, USA) according to the manufacturer's instructions and quantified with NanoDrop (Thermo Scientific, DE, USA). 1 µg of total RNA was pre-treated with Dnase I (Sigma-Aldrich, Milan, Italy) and used for cDNA synthesis

with the SMARTScribe Reverse Transcriptase (Clontech Laboratories, Mountain View, CA, USA). The following primers were used to analyse the expression of SVCT1: forward 5'-GCCCCTGAACACCTCTCATA-3' and reverse 5'-ATGGCCAGCATGATAGGAAA-3'; SVCT2: forward 5'-TTCTGTGTGGGAATCACTAC-3' and reverse 5'-ACCAGAGAGGCCAATTAGGG-3'. Amplification of GAPDH was used for internal loading control.

The PCR reaction mixture was prepared with 100 nM of forward and reverse primers, 2X PCR Master Mix Kit (DIATHEVA, Fano, Italy) and 50 ng of cDNA for each sample. The PCR conditions were one cycle at 95 °C for 8 min, 35/40 cycles at 95 °C for 15 s, 57 °C for 45 s, and 72 °C for 45 s and one final cycle at 72°C for 7 min. Amplification products were examined by electrophoresis on 1.5–2% agarose gels and visualized with ethidium bromide.

2.12 Analysis of mitochondrial superoxide formation with MitoSOX red

C2C12 Mb and Mt were grown in 35 mm tissue culture dishes containing an uncoated coverslip, exposed to AA in the presence of 0.1 mM DTT to prevent oxidation, washed with saline A and incubated for 30 min with 5 µM MitoSOX red. Cells were then washed twice with saline A and treated for 15 min with 2.5 µM arsenite in the absence or presence of 100 µM ATP. The cells were finally washed three times and fluorescence images were captured with a BX-51 microscope (Olympus, Milan, Italy), equipped with a SPOT-RT camera unit (Diagnostic Instruments, Delta Sistemi, Rome, Italy) using an Olympus LCAch 40 x/0.55 objective lens. The excitation and emission wavelengths were 510 and 580 nm respectively, with a 5-nm slit width for both emission and excitation. Images were collected with exposure times of 100-400 ms, digitally acquired and processed for fluorescence determination at the single cell level on a personal computer using Scion Image software (Scion Corp., Frederick, MD). Mean fluorescence values were determined by averaging the fluorescence values of at least 50 cells/treatment condition/experiment.

2.13 Measurement of mitochondrial Ca^{2+}

C2C12 Mb and Mt were grown in 35 mm tissue culture dishes containing an uncoated coverslip. Prior to experiments, the cells were pre-loaded (30 min) with 10 µM Rhod 2-acetoxymethyl ester, washed twice with saline A and finally treated for 15 min with arsenite in the absence or presence of ATP. The cells were finally washed three times and the fluorescence images were visualized using a fluorescence microscope. The resulting images were taken and processed as described above. The excitation and emission wavelengths were 540 and 590 nm, respectively, with a 5-nm slit width for both emission and excitation. Mean fluorescence values were determined by averaging the fluorescence values of at least 50 cells/treatment condition/experiment.

2.14 Statistical analysis

The results are expressed as means ± SD. Statistical differences were analysed by one-way ANOVA followed by Dunnett's test for multiple comparison or two-way ANOVA followed by Bonferroni's test for multiple comparison. A value of $P < 0.05$ was considered significant.

3. RESULTS

3.1 Differentiation of C2C12 myoblasts to myotubes.

C2C12 Mb were differentiated to Mt by growth in D-MEM supplemented with 1% serum. Under these conditions, these cells elongated and aligned each other within the first 24-48 h and, during the following days, multinucleated Mt were progressively formed. The progression of the differentiation process was monitored both at the morphological and biochemical levels. Fig. 1 shows the images of typical proliferating Mb (time 0, Fig. 1A) and differentiated Mt (day 4, Fig. 1B). Fig. 1 also provides evidence that Mt obtained under these conditions present specific markers of myogenic differentiation, as increased myogenin and myosin (Fig.1C) expression as well as increased CK activity (Fig.1D) and total protein content (Fig.1E), in comparison with Mb. Based on the above morphological and biochemical criteria, day 4 Mt presenting relevant characteristics of the differentiated skeletal muscle were employed in the experiments illustrated below.

3.2 Expression and activity of SVCT2 in Myoblasts and Myotubes

We investigated SVCT1 and 2 mRNA expression in Mb and Mt. U937 cells, which express both transporters [21, 42], were used as a positive control (C+, Fig. 2A). We found that Mb and Mt only express SVCT2 mRNA, and that the transcript was somewhat up-modulated in Mt. Western blot analysis produced results indicative of greater SVCT2 expression at the protein level in Mt than in Mb (Fig. 2B).

Transport studies performed at a 60 µM substrate concentration, revealed in the two cell types similar linear kinetics of AA uptake over a 60 min time-frame (Fig. 2C). The concentration-response curves for AA transport, hyperbolic in Mb and Mt (Fig. 2D), were characterized by the presence of a single kinetic component saturating at about 100 µM AA. Analysis of the transport data by the Eadie-Hofstee method (Fig. 2E) produced in the two cell types similar straight lines, allowing the calculation of apparent Km values of 27.60 ± 4.87 µM and 27.04 ± 4.81 µM in Mb and Mt, respectively. The Vmax values were also remarkably similar: 0.30 ± 0.014 and 0.27 ± 0.012 nmol/min/mg prot) in Mb and Mt, respectively.

Transport of AA was in both cell types Na^+- and temperature-dependent, since abolished under conditions in which the cation was replaced with choline, or when the uptake experiments were performed at ice-bath temperature (Fig. 2F). In addition, AA uptake in Mb and Mt was also suppressed by sulfinpyrazone (200 µM), as well as by PCMB (40 µM), two different SVCT inhibitors [43, 44].

3.3 Expression and activity of mitochondrial SVCT2 in Mb and Mt

In order to establish the expression of SVCT2 in Mb mitochondria, we performed experiments involving Western blot analyses of the Mc and Mp fractions, obtained as detailed in the Methods section. For comparison, SVCT2 expression was also tested in the cellular lysates as well as in other sub-cellular fractions. As show in Fig. 3A, there was evidence for SVCT2 expression in Mb

mitochondrial (Mc and Mp) (positive for cytocrome *c* and HSP-60) and PM (positive for GLUT3) fractions. The Mp fraction was however negative for GLUT3, thereby implying that the mitochondrial immunoreactivity to the anti-SVCT2 antibody was not due to a contamination of the PM fraction. The ER fraction was a contaminant of both the mitochondrial and PM fractions, and actin immunoreactivity was only present in the total lysate. It is however unlikely that such a contamination provides the anti-SVCT2 immunoreactivity to the Mc, Mp and plasma membrane fractions, since no anti-SVCT2 immunoreactivity was found in the ER-enriched fraction. Fig. 3B shows a representative image of the Mp fraction obtained with the TEM technique. The enrichment of mitochondria characterised by a fairly good integrity and without heavy contaminations due to other fractions can be clearly appreciated.

Collectively, these results provide evidence for the mitochondrial expression of SVCT2 in Mb. We next performed confocal microscopy studies using Mb labelled with anti-SVCT2 antibodies and with a mitochondrial probe, MitoTracker red (CMXRos). Fig. 4 (A-D) provides the image of single cells, however representative of the remaining cells in which the green identified the presence of SVCT2 (A), the red the mitochondria (B) and the yellow the co-localized pixels in the overlay image (C). Co-localization was determined with the Image J software, where background and threshold were set, generating a co-localization image (co-localized pixels in white) (D). Quantitative co-localization analysis (E) was made by determining the Pearson's correlation coefficient (P) and the Mander's overlap coefficients (M1 and M2) [45]. As shown in the Figure, the existence of a high level of co-localization of the two fluorophores (P = 0.57, M1 = 0.75, M2 = 0.89) is consistent with the notion that SVCT2 is expressed in C2C12 Mb mitochondria. In a single experiment, representative of three, the signal of co-localization was detected in >90% of the 135 Mb analyzed; an appreciable extra-mitochondrial SVCT2 green signal, diffused in the cytosol, was instead detected in only 20% of the cells. Hence, most of the SVCT2 detected in these cells appears to be localized in mitochondria.

We finally examined the kinetic properties of mitochondrial SVCT2 by performing transport studies in mitochondria isolated from proliferating Mb. Time-course analysis of AA uptake using a 100 µM substrate concentration, revealed that mitochondria take up the vitamin at a constant rate, for at least 15 min (Fig. 5A). The concentration response-curve obtained under these conditions (Fig. 5B) was hyperbolic and approached saturation at AA concentrations greater than 400 µM. Analysis of the transport data by the Eadie-Hofstee method (Fig. 5C) produced a straight line (r^2=0.91), consistent with the presence of a single functional component, allowing the calculation of an apparent Km of 273.0 ± 17.31 µM and a Vmax of 0.2821 ± 0.0278 nmol/min/mg prot. Transport of AA (250 µM) was abolished by sodium omission, incubation at ice-bath temperature as well as by sulfinpyrazone or PCMB (Fig. 5D).

The above experiments provide convincing experimental evidence for a significant expression of low affinity mitochondrial SVCT2 in C2C12 Mb.

We therefore addressed the question of whether mitochondrial SVCT2 expression and function is maintained during the early myoblast fusion. As expected, this was the more complex part of the study, as the problems encountered for the isolation of mitochondria from Mt were remarkably more significant than those experienced with Mb. Indeed, we obtained evidence for SVCT2 expression in the Mc, Mp and PM fractions (Fig. 6A). A very low signal was detected in the ER fraction, possibly dependent on the mitochondrial contamination. Indeed, anti-cytochrome *c* and anti-calnexin antibodies heavily marked both the ER and the mitochondrial fractions (Mc and Mp). Actin immunoreactivity was only detected in the cell lysate. The existence of a cross-contamination of the mitochondrial and ER fractions is also demonstrated by TEM analysis of the Mc fraction (Fig. 6B). This figure documents the presence of a large number of intact mitochondria along with some membrane fragments, derived from broken mitochondria and PM, as well as ribosomes derived from the ER. The image shown in Fig. 6C, is representative of the Mp fraction, which appears further enriched in mitochondria with however some residual damaged organelles and small fragments of the ER.

We also performed AA uptake studies in mitochondria isolated from Mt, but obtained inconclusive results. In these experiments, while concentration-dependent, ^{14}C-AA uptake was insensitive to Na^+ omission, temperature modulation and to the effects of SVCT2 inhibitors (not shown), thereby implying the existence of a non-specific binding of the vitamin to contaminating components of the purified mitochondrial preparations.

These results therefore demonstrate the PM expression of SVCT2 in C2C12-derived Mt. The results obtained are also consistent with the mitochondrial expression of the transporter, but nevertheless further experimental evidence is necessary to univocally establish this notion. In order to obtain definitive information in this direction, we performed confocal microscopy analyses of Mt labelled with an anti-SVCT2 antibody and MitoTracker red. These cells presented heterogeneous levels of differentiation as well as different expression of the mitochondrial SVCT2 (Fig. 7). A more detailed analysis of these images allowed us to formulate the following considerations and conclusions:

- cells with 1 nucleus are normally characterized by the mitochondrial expression of SVCT2 (signal of co-localization >90%). This was also true in cells presenting evidence of differentiation, *i.e.*, the presence of pseudo-filaments (Fig. 7A-B).

- the mitochondrial expression of SVCT2 is preserved in some Mt with 2 nuclei (about 75%) or even 3 nuclei, although in these cells there was evidence of somewhat reduced mitochondrial expression of the transporter. In some circumstances, however, an extra-mitochondrial signal was also noted (Fig. 7C-G). The arrows indicate the different localization of the green signal. It is difficult to compare the relative expression of mitochondrial SVCT2 in these cells with that previously detected in Mb, since the two cell types present remarkably different morphologies.

- Mt with more than 3 nuclei generally displayed a weak mitochondrial signal for SVCT2 (Fig. 7H, I).

- Experiments using day 7 Mt demonstrated that these cells display significantly lower overall SVCT2 expression than day 4 Mt. Most importantly, there was clear evidence of a dramatically reduced expression of the transporter in the mitochondria of day 7 Mt (Fig. 7 J-M).

These results collectively indicate that Mt obtained at day 4 of differentiation, characterised by a significant heterogeneity and an overall elevated SVCT2 expression, maintain the mitochondrial expression of the transporter in the very early stage of differentiation (*i.e.*, Mt with 1 or 2 nuclei). However, it appears that a progressive loss of mitochondrial SVCT2 expression ensues in parallel with the extent of Mt differentiation. This notion is further supported by the extremely low, or even undetectable expression of the transporter observed in the mitochondria of day 7 multinucleated Mt.

Based on these considerations, AA transport studies in the mitochondria of day 4 Mt appear not only complicated by the isolation process of these organelles, but also by the reduced expression of the transporter. We therefore made an attempt to at least obtain some indirect evidence of this transport activity from functional studies performed in intact cells, in particular since Mb and Mt are characterised by similar SVCT2-dependent transport and cellular accumulation of AA. Hence, if similar cellular accumulation of the vitamin is accompanied by a different mitochondrial uptake then, it should be possible to determine differential scavenging effects against mitochondrial ROS.

We reasoned that, in order to avoid misleading results, mitochondrial superoxide formation should be generated in the absence of oxidative effects in the extra-mitochondrial compartment, as oxidation of intracellular AA to DHA would eventually promote its mitochondrial uptake through hexose transporters. Under these conditions, prompt intra-mitochondrial reduction back of DHA to AA would then also lead to scavenging of mitochondrial ROS.

We therefore decided to use an experimental paradigm associated with the selective and exclusive formation of mitochondrial superoxide, recently developed in our laboratory. This experimental system is based on the notion that a limiting factor for mitochondrial superoxide formation induced by arsenite in U937 cells is represented by the mobilization of Ca^{2+} from the ER and the ensuing mitochondrial accumulation of the cation [46]. Consistently, low concentrations of, short exposure times to, arsenite are necessary and sufficient to promote maximal superoxide formation under conditions in which mitochondrial Ca^{2+} accumulation is induced by other treatments [47].

We therefore replicated our previous experiments obtained in U937 cells in both Mb and Mt, measuring mitochondrial superoxide formation (Fig. 8A, Mb; Fig. 8B, Mt) and mitochondrial Ca^{2+} accumulation (inset to Fig. 8A, Mb; inset to Fig. 8B, Mt), as detailed in the Methods section. The specificity of the probes employed in these experiments has been addressed in detail in previous studies [46, 48, 49]

As expected, we found that a 15 min exposure to 2.5 μM arsenite fails to promote these responses in both Mb and Mt. ATP, an agonist leading to mobilization of Ca^{2+} from the inositol-1,4,5-trisphosphate receptor (IP_3R) [50], instead promoted identical mitochondrial Ca^{2+} accumulation in the two cell types, however in the absence of ROS formation. It was then interesting to observe that the cocktail arsenite/ATP, while maintaining the ability to increase mitochondrial Ca^{2+} levels, also caused extensive mitochondrial superoxide formation, once again identical in the two cell types. Ru360, an inhibitor of the mitochondrial Ca^{2+} uniporter [51], while preventing mitochondrial Ca^{2+} accumulation, provoked a parallel inhibition of mitochondrial superoxide formation induced by arsenite/ATP in both cell types.

These results provide an indication that Mb and Mt are equally susceptible to the short-term effects of arsenite on the mitochondrial machinery resulting in Ca^{2+}-dependent superoxide formation under conditions in which the mitochondrial accumulation of the cation is enforced with an IP_3R agonist.

We therefore moved to experiments in which Mb and Mt were preloaded with increasing concentrations of AA, using the same conditions employed in uptake studies illustrated in Fig. 2, and then exposed to arsenite/ATP. We found that pre-exposure to low AA concentrations abolish mitochondrial superoxide formation induced by the cocktail arsenite/ATP in Mb, with hardly any effect being detected in Mt, even doubling the concentration of the vitamin promoting complete ROS inhibition in Mb (Fig. 8C). We also performed experiments in which the cells were exposed for increasing time intervals to 60 μM AA prior to treatment with arsenite/ATP. Under the same conditions, the 10 min exposure to AA was sufficient to promote complete ROS scavenging in Mb,

but the vitamin nevertheless failed to promote significant effects in Mt (Fig. 8D). A barely detectable, if any, inhibitory effect was observed only after 120 min of AA pre-exposure.

Collectively, the results presented in this study indicate that the progression of Mb to early Mt is characterised by a slight increase in the overall expression of SVCT2, with minor consequences on the PM transport of the vitamin, but nevertheless -at least based on findings from functional studies- with dramatic consequences on its accumulation in mitochondria. Since the expression of SVCT2 was in any case well preserved in early Mt, our functional studies are consistent with possibility that a loss of function of the transporter precedes the observed loss of expression detected in multinucleated day 7 Mt.

4 DISCUSSION

We investigated the expression and function of SVCT2 in the plasma and mitochondrial membranes of C2C12 Mb and early Mt. Studies at the mRNA and protein levels provided evidence for a significant expression of SVCT2 in both cell types, in the absence of detectable expression of SVCT1. These results are in line with previous findings obtained in C2C12 Mb and Mt [34, 52], as well as in slow skeletal myofibers from developing chicks and other adult mammals [53].

We also found that the differentiation protocol employed in our study resulted in early Mt characterized by increased SVCT2 transcript and protein expression. These findings are consistent with previous results from Sandoval et al. [34], providing evidence for a biphasic response, in which increased SVCT2 expression was detected in early Mt, with a progressively reduced expression occurring during further Mt growth. While our study did not specifically address this issue, the confocal images of day 7 Mt nevertheless demonstrate very low overall SVCT2 expression, thereby confirming the notion of decreased SVCT2 expression in late, multinucleated Mt.

The reduced expression of SVCT2 detected at day 7 of differentiation probably indicates that a high rate active transport of the vitamin is not necessary in cells characterized by low basal metabolic

activity and basal rate of ROS production. Besides, the amount of vitamin C found in the skeletal muscle is not particularly high in comparison with that detected in other tissues, in particular those characterized by a higher metabolic activity [25, 54]. Hence, our results may suggest that vitamin C slowly accumulates in these cells under resting conditions, and eventually exerts its antioxidant functions during ROS emission associated with contraction and physical activity. In addition, it can also be speculated that extensive ROS formation and the ensuing oxidation of extracellular AA, will promote efficient high capacity transport of DHA through hexose transporters.

The observation that SVCT2 up-regulation accompanies the process of early Mb fusion is instead compatible with a role of AA in the differentiation process, as suggested by Mitsumoto et al. [55]. While this issue should be specifically addressed in future studies, a role of vitamin C in the differentiation process has also been demonstrated in various other cell types [43, 56-61].

Our initial studies measuring AA transport in Mb and early Mt indicate that the differentiation process, while accompanied by an increased SVCT2 expression, nevertheless failed to significantly impact on the PM transport of the vitamin. Rather, the rate of AA uptake was somewhat lower in Mt than in Mb, and was indeed characterised by a 10% decrease in the Vmax, with no apparent change in affinity.

The significance of these findings is of complex interpretation, since Mb and Mt are completely different cells, with remarkable differences in their structural organization, function and morphology. The results from uptake studies were therefore calculated by normalizing the data to the protein content, and not to the cell number. Hence, the dichotomy existing between the increased SVCT2 expression and the reduced Vmax of early Mt is possibly attributable to their remarkably increased surface and, at least in principle, to specific changes in the subcellular distribution of the transporter. A correct interpretation of the above findings would then be that, despite the dramatic changes occurring during differentiation, early Mt maintain, in comparison with Mb, similar expression of SVCT2 and ability to take up AA.

We then moved to mitochondria and initially performed Western blot studies to determine the expression of SVCT2 in these and other subcellular compartments. Using specific markers, we also established the purity of the different subcellular fractions and obtained evidence for SVCT2 expression in mitochondria and in the PM, but not in the ER. The purity of the mitochondrial fractions, in particular the one using further centrifugation of the crude mitochondrial fraction on a Percoll gradient (Mp), was confirmed using the TEM technique. Confocal microscopy studies also provided an indication of a very large mitochondrial expression of SVCT2. We finally examined the kinetic properties of mitochondrial SVCT2 by performing transport studies in mitochondria isolated from proliferating Mb and measured kinetic parameters indicative of a SVCT2-dependent transport characterised by a low affinity for AA.

The reduced affinity of the mitochondrial SVCT2 is likely attributable to the need of high concentrations of specific cations, as Na^+ or Ca^{2+}, for optimal transport activity. These requirements are met in the case of the plasma membrane SVCT2, but not for the mitochondrial SVCT2, since the intracellular concentrations of Na^+ or Ca^{2+} are respectively one and four order of magnitude lower than those normally present in the extracellular milieu [62].

Thus, undifferentiated/proliferating C2C12 Mb express functional SVCT2 in their mitochondria, thereby suggesting that an active transport of AA, although with low affinity, is necessary to provide adequate amounts of the vitamin to these organelles. We speculate that the mitochondrial respiratory activity necessary to support Mb proliferation is associated with the formation of large amounts of mitochondrial ROS. An elevated expression of mitochondrial SVCT2 is therefore functional for an adequate supply of vitamin C, thereby contributing to the antioxidant defence of these organelles.

It is well established that the differentiation of Mb to Mt is accompanied by the formation of a complex network between the mitochondria and the sarcoplasmic reticulum, which complicates the process of isolation of mitochondria [63]. In the skeletal muscle, the mitochondria create a three-dimensional network around the sarcomeres [64] and retain functional interactions with lipid droplets and the cytoskeleton. The interaction with the sarcoplasmic reticulum is based on a system defined

as mitochondria associated membranes, very difficult to remove during the process of mitochondria isolation [65, 66].

We encountered these problems also using the more selective isolation procedure of mitochondria, obtaining clear evidence for a significant cross-contamination of this fraction with the ER and possibly the PM, using both Western blot and TEM techniques. Likewise, the poor purity of the mitochondria made our attempts to measure AA transport unsuccessful. We could however obtain reliable information from confocal microscopy studies, allowing the detection of SVCT2 also in Mt mitochondria, in which the expression of the transporter appeared inversely related to the number of nuclei per Mt, a parameter indicative of the degree of differentiation. More specifically, a very large proportion of cells with one nucleus, even in the presence of pseudo-filaments, was characterised by the mitochondrial expression of SVCT2. Similar observations were made in cells with two nuclei. While it would be difficult to establish whether this localization was comparable to, or lower than, that found in Mb, it appears however clear that the level of SVCT2 expression was progressively reduced in cells with three or more nuclei. This notion was even more clearly established in multinucleated day 7 Mt.

The progressive reduction in the expression of SVCT2 detected in the mitochondria of non-proliferating Mt, somehow anticipating an overall reduced cellular expression of the transporter, likely reflects a reduced mitochondrial requirement of the vitamin, due to low mitochondrial ROS production. We speculate that, although this notion can be more directly established experimentally, something similar takes place *in vivo*, in skeletal muscle cell mitochondria. Under these conditions, however, mitochondria will nevertheless slowly accumulate the vitamin to cope with episodic conditions associated with extensive ROS emission, *i.e.*, during intense physical activity.

The final experiments, taking advantage of the similar cellular uptake of the vitamin in Mb and Mt, and of the use of a system selectively generating equal levels of mitochondrial superoxide, addressed the issue of whether a different mitochondrial accumulation of AA can be inferred from a different superoxide scavenging. The outcome of the experiments performed in Mb was in line with the uptake

studies, as a short-term pre-exposure to low concentrations of the vitamin abolished mitochondrial superoxide formation. The dramatic difference in the results obtained in day 4 Mt was instead unexpected, since a moderately reduced protective response afforded by pre-incubation to AA would have been more compatible with the results of confocal microscopy studies, providing evidence of a fairly good, or at the most slightly reduced, expression of mitochondrial SVCT2. In fact, our experiments failed to provide evidence for a protective effect of AA in these cells. The lack of a protective response was observed also using greater concentrations, or longer times of exposure to the vitamin, than those affording complete protection in Mb experiments.

These results therefore demonstrate that early Mt, while effectively accumulating AA, fail to transport the vitamin in their mitochondria for reasons that can be only partially explained by the reduced SVCT2 expression. In fact, based on the results from functional assays, the residual fraction of SVCT2 was able to transport very small amounts of AA in mitochondria, thereby implying the possibility of a loss of function.

The results presented in this study can be summarized as detailed in the scheme reported in Fig. 9. Proliferating Mb express SVCT2 in both the plasma and mitochondrial membranes, and transport the vitamin with a high and low affinity, respectively. The triggering of the differentiation of Mb to Mt is paralleled by an early up-regulation of SVCT2, with an apparently minor impact on the cellular transport of the vitamin. Hence, despite the dramatic changes and increase in size occurring during differentiation, early Mt nevertheless maintain an adequate expression of SVCT2 and ability to take up AA from the extracellular milieu, eventually necessary to support differentiation and possibly other events. Further differentiation of these cells to late Mt resulted in a significantly decreased expression of mitochondrial SVCT2, thereby implying a reduced ability of these organelles to take up AA. However, a severely compromised transport of AA, as inferred from functional studies, takes place also in early Mt, characterised by a significant residual mitochondrial expression of SVCT2, thereby raising doubts on its biological activity even at this stage of the differentiation process.

Declaration of Competing Interest

The authors declare no conflicts of interest.

Funding

This work was supported by Ministero dell'Università e della Ricerca Scientifica e Tecnologica, Programmi di Ricerca Scientifica di Rilevante Interesse Nazionale, 2015, [Grant number: 2015MJBEM2-003. O.C.].

Supplementary data

Supplementary data associated with this article can be found in the online version.

Acknowledgements

The authors thank Dr. Antonella Antonelli for helpful advice and technical support.

REFERENCES

[1] B. Frei, L. England, B.N. Ames, Ascorbate is an outstanding antioxidant in human blood plasma, Proc Natl Acad Sci U S A 86(16) (1989) 6377-81.

[2] C.J. Fuller, S.M. Grundy, E.P. Norkus, I. Jialal, Effect of ascorbate supplementation on low density lipoprotein oxidation in smokers, Atherosclerosis 119(2) (1996) 139-50.

[3] Y. Tamari, H. Nawata, E. Inoue, A. Yoshimura, H. Yoshii, G. Kashino, M. Seki, T. Enomoto, M. Watanabe, K. Tano, Protective roles of ascorbic acid in oxidative stress induced by depletion of superoxide dismutase in vertebrate cells, Free Radic Res 47(1) (2013) 1-7.

[4] H. Tsukaguchi, T. Tokui, B. Mackenzie, U.V. Berger, X.Z. Chen, Y. Wang, R.F. Brubaker, M.A. Hediger, A family of mammalian Na+-dependent L-ascorbic acid transporters, Nature 399(6731) (1999) 70-5.

[5] A. Godoy, V. Ormazabal, G. Moraga-Cid, F.A. Zuniga, P. Sotomayor, V. Barra, O. Vasquez, V. Montecinos, L. Mardones, C. Guzman, M. Villagran, L.G. Aguayo, S.A. Onate, A.M. Reyes, J.G. Carcamo, C.I. Rivas, J.C. Vera, Mechanistic insights and functional determinants of the transport cycle of the ascorbic acid transporter SVCT2. Activation by sodium and absolute dependence on bivalent cations, J Biol Chem 282(1) (2007) 615-24.

[6] J.C. Vera, C.I. Rivas, J. Fischbarg, D.W. Golde, Mammalian facilitative hexose transporters mediate the transport of dehydroascorbic acid, Nature 364(6432) (1993) 79-82.

[7] S.C. Rumsey, O. Kwon, G.W. Xu, C.F. Burant, I. Simpson, M. Levine, Glucose transporter isoforms GLUT1 and GLUT3 transport dehydroascorbic acid, J Biol Chem 272(30) (1997) 18982-9.

[8] G. Banhegyi, A. Benedetti, E. Margittai, P. Marcolongo, R. Fulceri, C.E. Nemeth, A. Szarka, Subcellular compartmentation of ascorbate and its variation in disease states, Biochim Biophys Acta 1843(9) (2014) 1909-16.

[9] O. Cantoni, A. Guidarelli, M. Fiorani, Mitochondrial Uptake and Accumulation of Vitamin C: What Can We Learn from Cell Culture Studies?, Antioxid Redox Signal 29(15) (2018) 1502-1515.

[10] M. Fiorani, A. Guidarelli, O. Cantoni, Mitochondrial Reactive Oxygen Species: The effects of Mitochondrial Ascorbic Acid vs untargeted and Mitochondria-targeted antioxidants, International Journal of Radiation Biology (2020) 1-25.

[11] S.J. Padayatty, A. Katz, Y. Wang, P. Eck, O. Kwon, J.H. Lee, S. Chen, C. Corpe, A. Dutta, S.K. Dutta, M. Levine, Vitamin C as an antioxidant: evaluation of its role in disease prevention, J Am Coll Nutr 22(1) (2003) 18-35.

[12] S. Singh, S.V. Rana, Ascorbic acid improves mitochondrial function in liver of arsenic-treated rat, Toxicol Ind Health 26(5) (2010) 265-72.

[13] M.G. Traber, J.F. Stevens, Vitamins C and E: beneficial effects from a mechanistic perspective, Free Radic Biol Med 51(5) (2011) 1000-13.

[14] O.C. Ingebretsen, P.T. Normann, Transport of ascorbate into guinea pig liver mitochondria, Biochim Biophys Acta 684(1) (1982) 21-6.

[15] X. Li, C.E. Cobb, K.E. Hill, R.F. Burk, J.M. May, Mitochondrial uptake and recycling of ascorbic acid, Arch Biochem Biophys 387(1) (2001) 143-53.

[16] K. Ramanathan, S. Shila, S. Kumaran, C. Panneerselvam, Ascorbic acid and alpha-tocopherol as potent modulators on arsenic induced toxicity in mitochondria, J Nutr Biochem 14(7) (2003) 416-20.

[17] Y. Fujimoto, M. Matsui, T. Fujita, The accumulation of ascorbic acid and iron in rat liver mitochondria after lipid peroxidation, Jpn J Pharmacol 32(2) (1982) 397-9.

[18] G.T. Vatassery, W.E. Smith, H.T. Quach, J.C. Lai, In vitro oxidation of vitamin E, vitamin C, thiols and cholesterol in rat brain mitochondria incubated with free radicals, Neurochem Int 26(5) (1995) 527-35.

[19] A. Szarka, T. Lorincz, [Cellular and intracellular transport of vitamin C. The physiologic aspects], Orv Hetil 154(42) (2013) 1651-6.

[20] S. Kc, J.M. Carcamo, D.W. Golde, Vitamin C enters mitochondria via facilitative glucose transporter 1 (Glut1) and confers mitochondrial protection against oxidative injury, FASEB J 19(12) (2005) 1657-67.

[21] C. Azzolini, M. Fiorani, L. Cerioni, A. Guidarelli, O. Cantoni, Sodium-dependent transport of ascorbic acid in U937 cell mitochondria, IUBMB Life 65(2) (2013) 149-53.

[22] C. Munoz-Montesino, F.J. Roa, E. Pena, M. Gonzalez, K. Sotomayor, E. Inostroza, C.A. Munoz, I. Gonzalez, M. Maldonado, C. Soliz, A.M. Reyes, J.C. Vera, C.I. Rivas, Mitochondrial ascorbic acid transport is mediated by a low-affinity form of the sodium-coupled ascorbic acid transporter-2, Free Radic Biol Med 70 (2014) 241-54.

[23] J.S. Yin, Y. Zhang, N. Xua, T. Wang, H., A fluorophore-conjugated ascorbic acid functions for the visualization of sodium vitamin C transporters in living cells, Anal. Methods 7 (2015) 9663-9672.

[24] E. Pena, F.J. Roa, E. Inostroza, K. Sotomayor, M. Gonzalez, F.A. Gutierrez-Castro, M. Maurin, K. Sweet, C. Labrousse, M. Gatica, C.F. Aylwin, P. Mendoza, M. Maldonado, C. Delgado, J. Madariaga, J. Panes, T. Silva-Grecchi, Concha, II, G. Moraga-Cid, A.M. Reyes, C. Munoz-Montesino, J.C. Vera, C.I. Rivas, Increased expression of mitochondrial sodium-coupled ascorbic acid transporter-2 (mitSVCT2) as a central feature in breast cancer, Free Radic Biol Med 135 (2019) 283-292.

[25] R. Schaus, The ascorbic acid content of human pituitary, cerebral cortex, heart, and skeletal muscle and its relation to age, Am J Clin Nutr 5(1) (1957) 39-41.

[26] S.T. Omaye, E.E. Schaus, M.A. Kutnink, W.C. Hawkes, Measurement of vitamin C in blood components by high-performance liquid chromatography. Implication in assessing vitamin C status, Ann N Y Acad Sci 498 (1987) 389-401.

[27] A.C. Carr, S.M. Bozonet, J.M. Pullar, J.W. Simcock, M.C. Vissers, Human skeletal muscle ascorbate is highly responsive to changes in vitamin C intake and plasma concentrations, Am J Clin Nutr 97(4) (2013) 800-7.

[28] S.A. Mason, R. Baptista, P.A. Della Gatta, A. Yousif, A.P. Russell, G.D. Wadley, High-dose vitamin C supplementation increases skeletal muscle vitamin C concentration and SVCT2 transporter expression but does not alter redox status in healthy males, Free Radic Biol Med 77 (2014) 130-8.

[29] S.K. Powers, E.E. Talbert, P.J. Adhihetty, Reactive oxygen and nitrogen species as intracellular signals in skeletal muscle, J Physiol 589(Pt 9) (2011) 2129-38.

[30] K.J. Davies, A.T. Quintanilha, G.A. Brooks, L. Packer, Free radicals and tissue damage produced by exercise, Biochemical and biophysical research communications 107(4) (1982) 1198-205.

[31] S.A. Mason, P.A. Della Gatta, R.J. Snow, A.P. Russell, G.D. Wadley, Ascorbic acid supplementation improves skeletal muscle oxidative stress and insulin sensitivity in people with type 2 diabetes: Findings of a randomized controlled study, Free Radic Biol Med 93 (2016) 227-38.

[32] C. Schoneich, E. Dremina, N. Galeva, V. Sharov, Apoptosis in differentiating C2C12 muscle cells selectively targets Bcl-2-deficient myotubes, Apoptosis 19(1) (2014) 42-57.

[33] J. Tang, A. He, H. Yan, G. Jia, G. Liu, X. Chen, J. Cai, G. Tian, H. Shang, H. Zhao, Damage to the myogenic differentiation of C2C12 cells by heat stress is associated with up-regulation of several selenoproteins, Sci Rep 8(1) (2018) 10601.

[34] D. Sandoval, J. Ojeda, M. Low, F. Nualart, S. Marcellini, N. Osses, J.P. Henriquez, The vitamin C transporter SVCT2 is down-regulated during postnatal development of slow skeletal muscles, Histochem Cell Biol 139(6) (2013) 887-94.

[35] K. Koziel, M. Lebiedzinska, G. Szabadkai, M. Onopiuk, W. Brutkowski, K. Wierzbicka, G. Wilczynski, P. Pinton, J. Duszynski, K. Zablocki, M.R. Wieckowski, Plasma membrane associated membranes (PAM) from Jurkat cells contain STIM1 protein is PAM involved in the capacitative calcium entry?, Int J Biochem Cell Biol 41(12) (2009) 2440-9.

[36] M.R. Wieckowski, C. Giorgi, M. Lebiedzinska, J. Duszynski, P. Pinton, Isolation of mitochondria-associated membranes and mitochondria from animal tissues and cells, Nature protocols 4(11) (2009) 1582-90.

[37] S. Burattini, P. Ferri, M. Battistelli, R. Curci, F. Luchetti, E. Falcieri, C2C12 murine myoblasts as a model of skeletal muscle development: morpho-functional characterization, Eur J Histochem 48(3) (2004) 223-33.

[38] O. Cantoni, I. Tommasini, L. Cerioni, The arachidonate-dependent survival signaling preventing toxicity in monocytes/macrophages exposed to peroxynitrite, Methods Enzymol 441 (2008) 73-82.

[39] I. Savini, S. Duflot, L. Avigliano, Dehydroascorbic acid uptake in a human keratinocyte cell line (HaCaT) is glutathione-independent, Biochem J 345 Pt 3 (2000) 665-72.

[40] Determination of creatine-kinase activity in serum, 2010. http://biochemistry.semmelweis.hu/uploads/obi_okt_gra_en/obi_e_tananyag_en/obi_okt_gyakorlatok_en/obi_gya_en_creatine%20kinase.pdf.

[41] M.M. Bradford, A rapid and sensitive method for the quantitation of microgram quantities of protein utilizing the principle of protein-dye binding, Anal Biochem 72 (1976) 248-54.

[42] M. Scotti, M. Fiorani, A. Guidarelli, O. Cantoni, Differentiation of Promonocytic U937 Cells to Monocytes Is Associated with Reduced Mitochondrial Transport of Ascorbic Acid, Oxid Med Cell Longev 2018 (2018) 4194502.

[43] H. Qiao, J.M. May, Macrophage differentiation increases expression of the ascorbate transporter (SVCT2), Free Radic Biol Med 46(8) (2009) 1221-32.

[44] J.M.Q. May, Z.-C., Redox regulation of ascorbic acid transport: role of transporter and intracellular sulfhydryls, Biofactors 20 (2004) 199-211.

[45] J. Schindelin, I. Arganda-Carreras, E. Frise, V. Kaynig, M. Longair, T. Pietzsch, S. Preibisch, C. Rueden, S. Saalfeld, B. Schmid, J.Y. Tinevez, D.J. White, V. Hartenstein, K. Eliceiri, P. Tomancak, A. Cardona, Fiji: an open-source platform for biological-image analysis, Nat Methods 9(7) (2012) 676-82.

[46] A. Guidarelli, M. Fiorani, L. Cerioni, O. Cantoni, Calcium signals between the ryanodine receptor- and mitochondria critically regulate the effects of arsenite on mitochondrial superoxide formation and on the ensuing survival vs apoptotic signaling, Redox biology 20 (2019) 285-295.

[47] A. Guidarelli, L. Cerioni, M. Fiorani, A. Catalani, O. Cantoni, Arsenite-Induced Mitochondrial Superoxide Formation: Time and Concentration Requirements for the Effects of the Metalloid on the Endoplasmic Reticulum and Mitochondria, The Journal of pharmacology and experimental therapeutics 373(1) (2020) 62-71.

[48] P. Mukhopadhyay, M. Rajesh, G. Hasko, B.J. Hawkins, M. Madesh, P. Pacher, Simultaneous detection of apoptosis and mitochondrial superoxide production in live cells by flow cytometry and confocal microscopy, Nature protocols 2(9) (2007) 2295-301.

[49] A. Guidarelli, M. Fiorani, S. Carloni, L. Cerioni, W. Balduini, O. Cantoni, The study of the mechanism of arsenite toxicity in respiration-deficient cells reveals that NADPH oxidase-derived

superoxide promotes the same downstream events mediated by mitochondrial superoxide in respiration-proficient cells, Toxicol Appl Pharmacol 307 (2016) 35-44.

[50] K. Maes, L. Missiaen, P. De Smet, S. Vanlingen, G. Callewaert, J.B. Parys, H. De Smedt, Differential modulation of inositol 1,4,5-trisphosphate receptor type 1 and type 3 by ATP, Cell calcium 27(5) (2000) 257-67.

[51] C. Zazueta, M.E. Sosa-Torres, F. Correa, A. Garza-Ortiz, Inhibitory properties of ruthenium amine complexes on mitochondrial calcium uptake, Journal of bioenergetics and biomembranes 31(6) (1999) 551-7.

[52] I. Savini, M.V. Catani, G. Duranti, R. Ceci, S. Sabatini, L. Avigliano, Vitamin C homeostasis in skeletal muscle cells, Free Radic Biol Med 38(7) (2005) 898-907.

[53] M. Low, D. Sandoval, E. Aviles, F. Perez, F. Nualart, J.P. Henriquez, The ascorbic acid transporter SVCT2 is expressed in slow-twitch skeletal muscle fibres, Histochem Cell Biol 131(5) (2009) 565-74.

[54] S.J. Padayatty, M. Levine, Vitamin C: the known and the unknown and Goldilocks, Oral Dis 22(6) (2016) 463-93.

[55] Y. Mitsumoto, Z. Liu, A. Klip, A long-lasting vitamin C derivative, ascorbic acid 2-phosphate, increases myogenin gene expression and promotes differentiation in L6 muscle cells, Biochemical and biophysical research communications 199(1) (1994) 394-402.

[56] M. Low, D. Sandoval, B. Morales, F. Nualart, J.P. Henriquez, Up-regulation of the vitamin C transporter SVCT2 upon differentiation and depolarization of myotubes, FEBS Lett 585(2) (2011) 390-6.

[57] S. Fulzele, P. Chothe, R. Sangani, N. Chutkan, M. Hamrick, M. Bhattacharyya, P.D. Prasad, I. Zakhary, M. Bowser, C. Isales, V. Ganapathy, Sodium-dependent vitamin C transporter SVCT2: expression and function in bone marrow stromal cells and in osteogenesis, Stem Cell Res 10(1) (2013) 36-47.

[58] X. Wu, N. Itoh, T. Taniguchi, T. Nakanishi, Y. Tatsu, N. Yumoto, K. Tanaka, Zinc-induced sodium-dependent vitamin C transporter 2 expression: potent roles in osteoblast differentiation, Arch Biochem Biophys 420(1) (2003) 114-20.

[59] R. Sangani, C.D. Pandya, M.H. Bhattacharyya, S. Periyasamy-Thandavan, N. Chutkan, S. Markand, W.D. Hill, M. Hamrick, C. Isales, S. Fulzele, Knockdown of SVCT2 impairs in-vitro cell attachment, migration and wound healing in bone marrow stromal cells, Stem Cell Res 12(2) (2014) 354-63.

[60] P. Pastor, P. Cisternas, K. Salazar, C. Silva-Alvarez, K. Oyarce, N. Jara, F. Espinoza, A.D. Martinez, F. Nualart, SVCT2 vitamin C transporter expression in progenitor cells of the postnatal neurogenic niche, Front Cell Neurosci 7 (2013) 119.

[61] T. Caprile, K. Salazar, A. Astuya, P. Cisternas, C. Silva-Alvarez, H. Montecinos, C. Millan, M. de Los Angeles Garcia, F. Nualart, The Na^+-dependent L-ascorbic acid transporter SVCT2 expressed in brainstem cells, neurons, and neuroblastoma cells is inhibited by flavonoids, J Neurochem 108(3) (2009) 563-77.

[62] D.E. Clapham, Calcium signaling, Cell 131(6) (2007) 1047-58.

[63] S. Marchi, S. Patergnani, P. Pinton, The endoplasmic reticulum-mitochondria connection: one touch, multiple functions, Biochim Biophys Acta 1837(4) (2014) 461-9.

[64] T. Ogata, Y. Yamasaki, Ultra-high-resolution scanning electron microscopy of mitochondria and sarcoplasmic reticulum arrangement in human red, white, and intermediate muscle fibers, Anat Rec 248(2) (1997) 214-23.

[65] C. Giorgi, D. De Stefani, A. Bononi, R. Rizzuto, P. Pinton, Structural and functional link between the mitochondrial network and the endoplasmic reticulum, Int J Biochem Cell Biol 41(10) (2009) 1817-27.

[66] S. Patergnani, J.M. Suski, C. Agnoletto, A. Bononi, M. Bonora, E. De Marchi, C. Giorgi, S. Marchi, S. Missiroli, F. Poletti, A. Rimessi, J. Duszynski, M.R. Wieckowski, P. Pinton, Calcium signaling around Mitochondria Associated Membranes (MAMs), Cell Commun Signal 9 (2011) 19.

Figure 1. C2C12 Myoblasts and Myotubes. Representative images of Mb (A) and day 4 Mt (B). A, bar= 10 µm; B, bar= 20 µm. (C) Western blot analysis for myogenin and myosin expression in Mb and Mt. Actin was used as a loading control. (D) Creatine kinase activity of Mb and Mt. (E) Protein content of Mb and Mt. Results are the means ± SD of at least three separate experiments. **P*< 0.01, referred to the differences between Mb and Mt (one-way ANOVA followed by Dunnet's test).

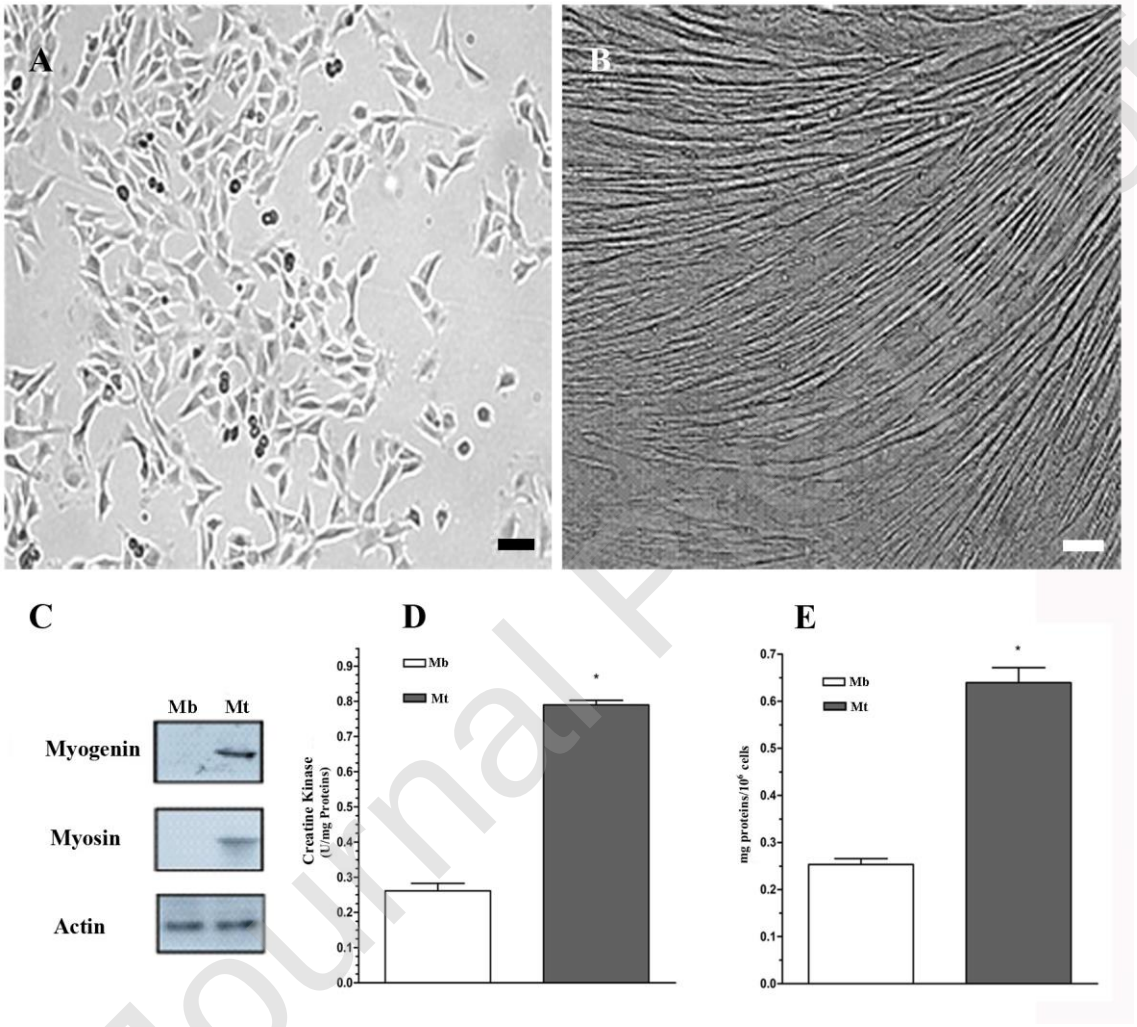

Figure 2. Analysis of SVCT2 expression and AA uptake in C2C12 Myoblasts and Myotubes. (A) RT-PCR analysis of SVCT1 and SVCT2 expression in Mb and Mt. U937 cells were used as a positive control for SVCT1 and SVCT2 expression (C+). (C-) is a no-template control. Glyceraldehyde 3-phosphate dehydrogenase (GAPDH) was used as a loading control. (B) Western blot analysis using antibodies against SVCT2 in Mb and Mt. The blot shown is representative of at

least 3 separate experiments with similar outcomes. Actin was used as a loading control. (C) Time-course of AA transport in Mb and Mt exposed to 60 μM AA in EB. (D) Dose-dependence of AA uptake (10 min) in Mb and Mt. (E) Eadie-Hofstee plot of the data reported in D. Values are the means of at least three independent experiments. (F) Mb and Mt were exposed to 60 μM AA at 37° C in the absence or presence of 200 μM sulfinpyrazone (S-pyr) or 40 μM PCMB. In other experiments, the extracellular medium was manipulated to replace Na^+ with choline. The uptake of AA was also determined after exposure to AA at 4° C. Results represent the means ± SD calculated from at least 3 separate experiments. *P< 0.01, as compared to the first bar of each set (one-way ANOVA followed by Dunnet's test).

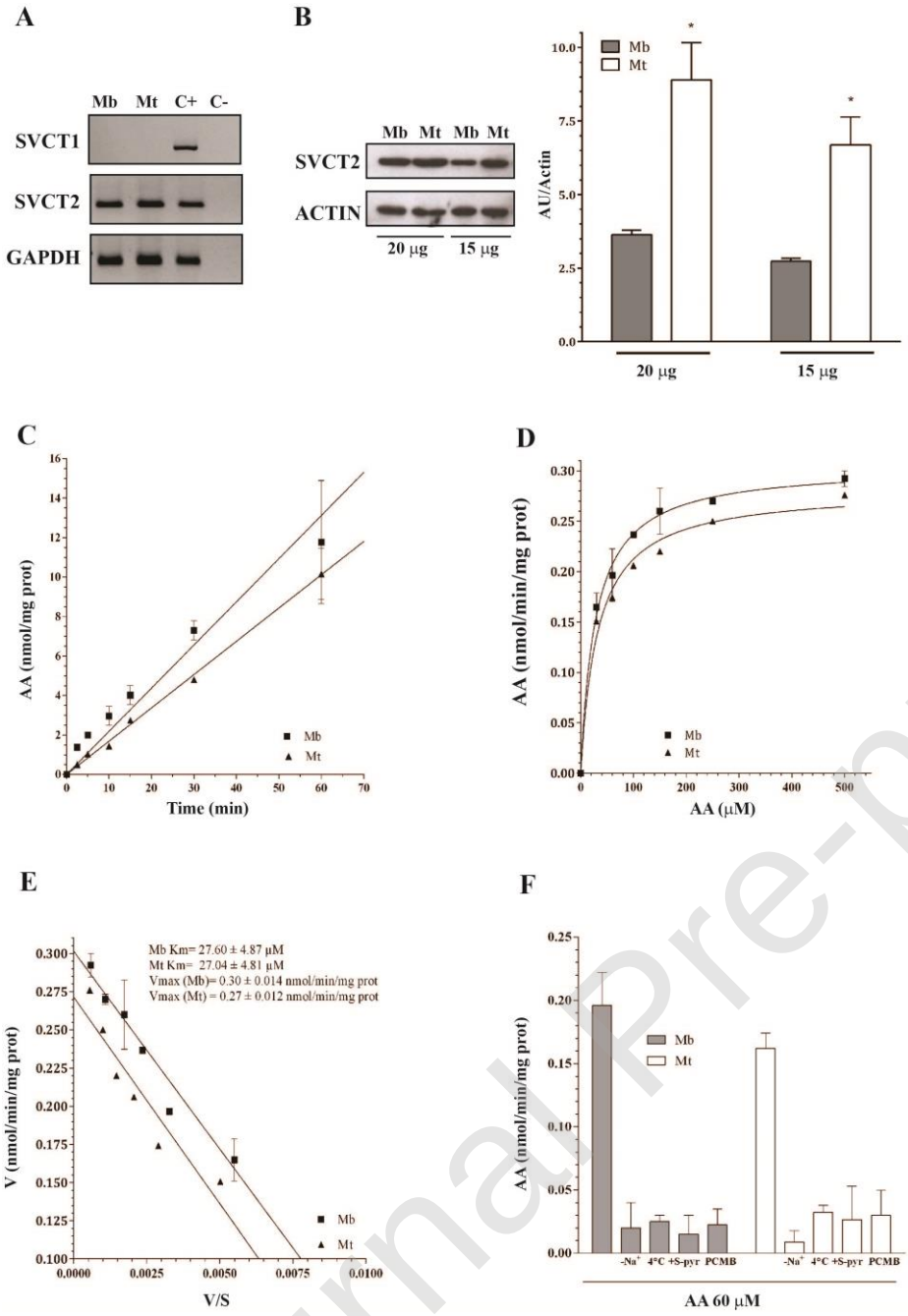

Figure 3. Mitochondrial expression of SVCT2 in C2C12 Myoblasts: assessment of the purity of the mitochondrial fraction. The cells were homogenized and fractionated by differential centrifugation and Percoll gradient technique. The fractions were separated by SDS-PAGE, transferred to PVDF membranes, and immunodetected with appropriate antibodies. (Tot: total homogenate; Mc: crude mitochondrial fraction; Mp: pure mitochondrial fraction; PM: plasma membrane; ER: endoplasmic reticulum). (B) TEM analysis of the Mp fraction. Bar = 0.5 µm; m= mitochondrion; * = empty mitochondrion.

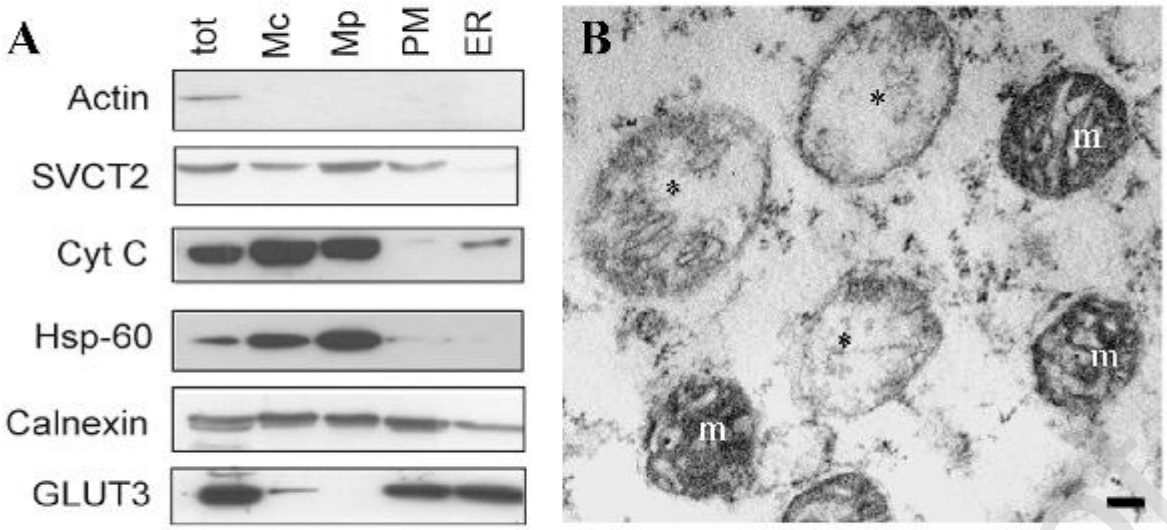

Figure 4. Mitochondrial localization of SVCT2 in C2C12 Myoblasts assessed by confocal microscopy. (A-D) Representative fluorescence images of cells double stained for SVCT2 (green, A) and mitochondria (MitoTracker Red, B). In the merged image (C) the co-localization appears yellow. (D) Co-localization analysis and quantification performed with Image J software. (E) The Pearson's (P) and Mander's (M1 and M2) overlap coefficients represented as the average of ten images. A-D, bar = 25 μm.

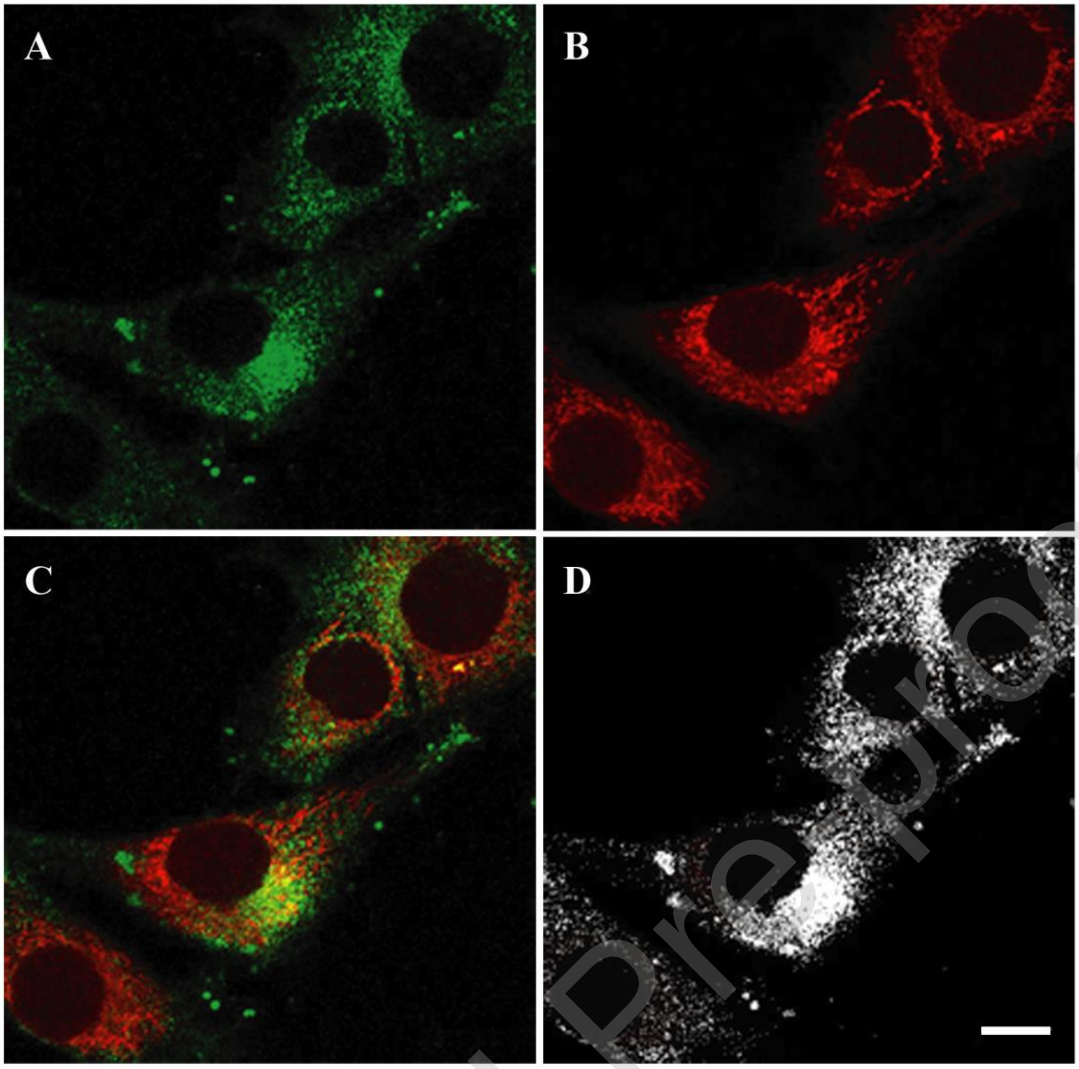

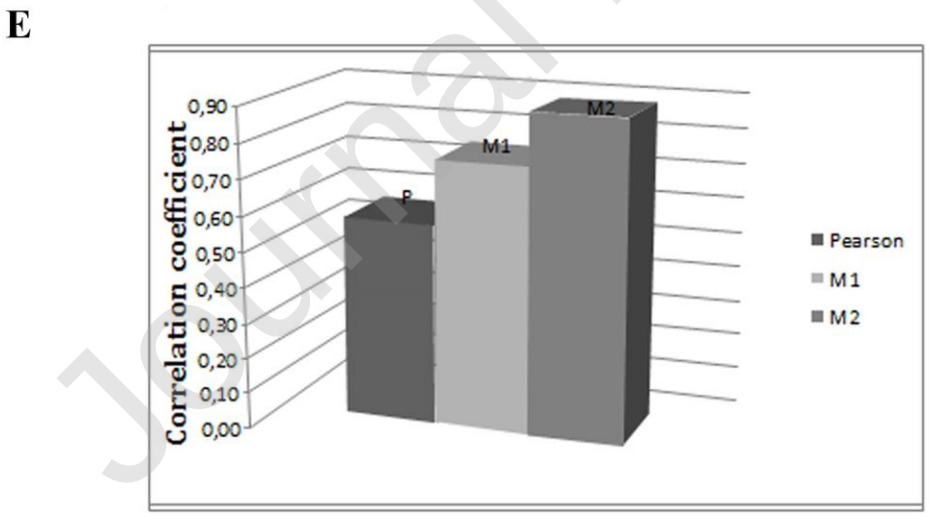

Figure 5. Kinetics of AA transport in mitochondria isolated from C2C12 Myoblasts. (A) Time-dependence of AA (100 µM) transport in mitochondria isolated from Mb. (B) Concentration-response curve for AA transport in isolated mitochondria. (C) Eadie-Hofstee plot of the data reported in (A).

(D) Mitochondria were exposed at 37° C to 250 µM AA alone or associated with 200 µM sulfinpyrazone (S-pyr) or 40 µM PCMB. In other experiments, the extramitochondrial medium was manipulated to replace Na^+ with choline. The uptake of AA was also determined after exposure to AA at 4° C. Values are the means of at least three independent experiments.

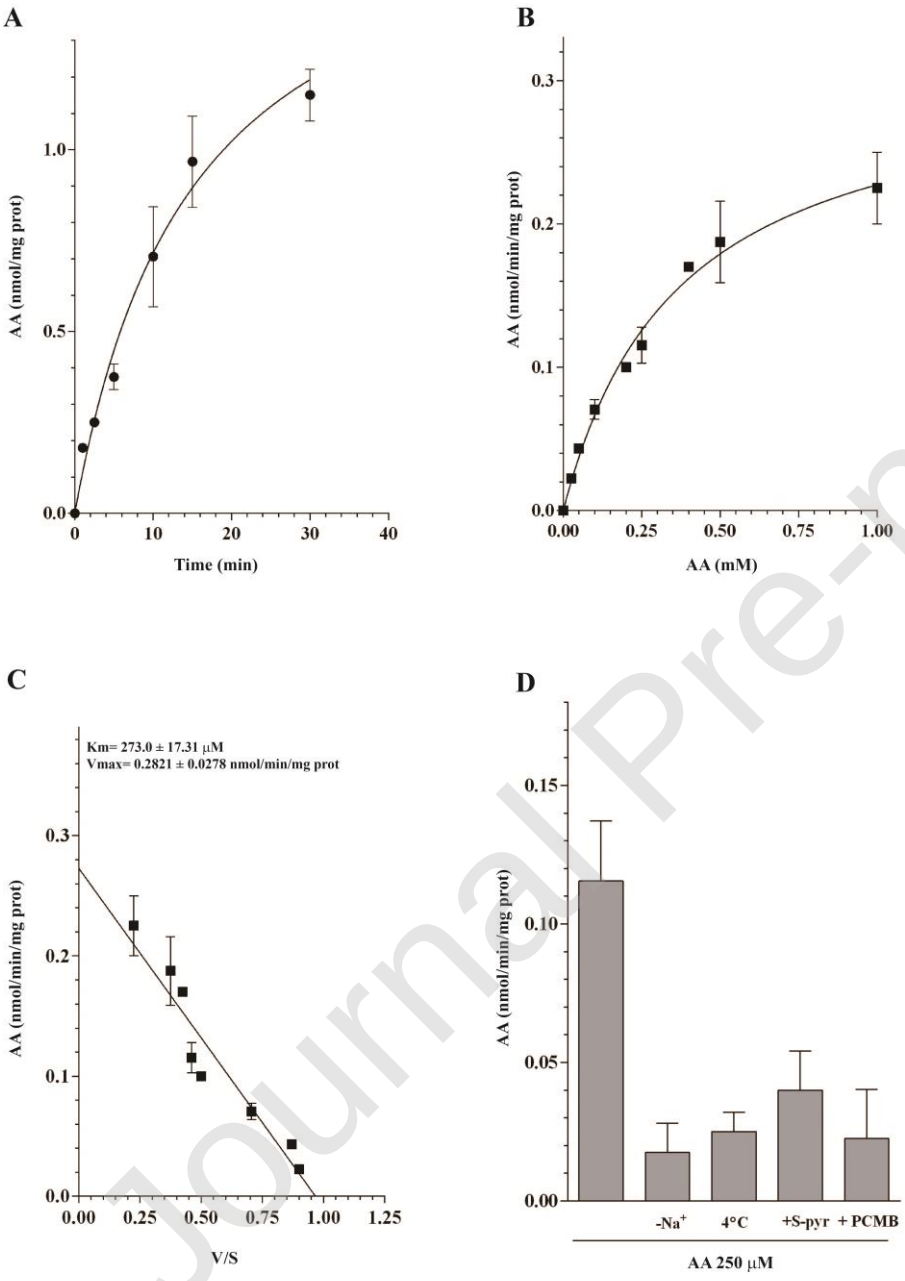

Figure 6. Mitochondrial expression of SVCT2 in C2C12 Myotubes: assessment of the purity of the mitochondrial fractions.

(A) The cells were homogenized and fractionated by the differential centrifugation and Percoll gradient techniques. The fractions were separated by SDS-PAGE, transferred to PVDF

membranes, and immunodetected with appropriate antibodies. (Tot: total homogenate; Mc: crude mitochondrial fraction; Mp: purified mitochondrial fraction; PM: plasma membrane; ER: endoplasmic reticulum). (B) TEM analysis of the total homogenate, bar= 1 µm; (C) TEM analysis of the crude mitochondrial fraction (Mc), bar = 0.2 µm. m = mitochondrion, → = PM and ER pieces.

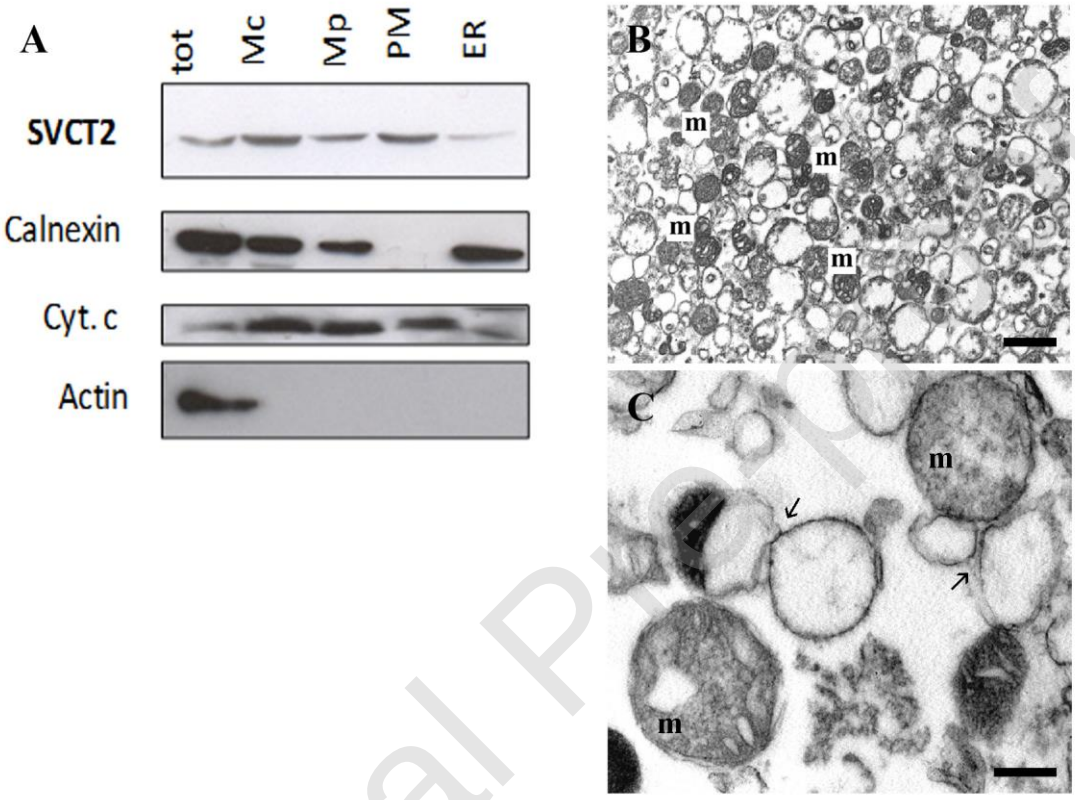

Figure 7. Mitochondrial localization of SVCT2 in C2C12 Myotubes assessed by confocal microscopy. Representative fluorescence images of Mt double stained for SVCT2 (green) and mitochondria (MitoTracker Red). In the merged images obtained with day 4 Mt (A-I) the co-localization appears yellow. 7-day Mt (J-M) displayed markedly reduced overall and mitochondrial expression of SVCT2. A, B, H-M, Bar= 10 µm; C-G, Bar= 5 µm.

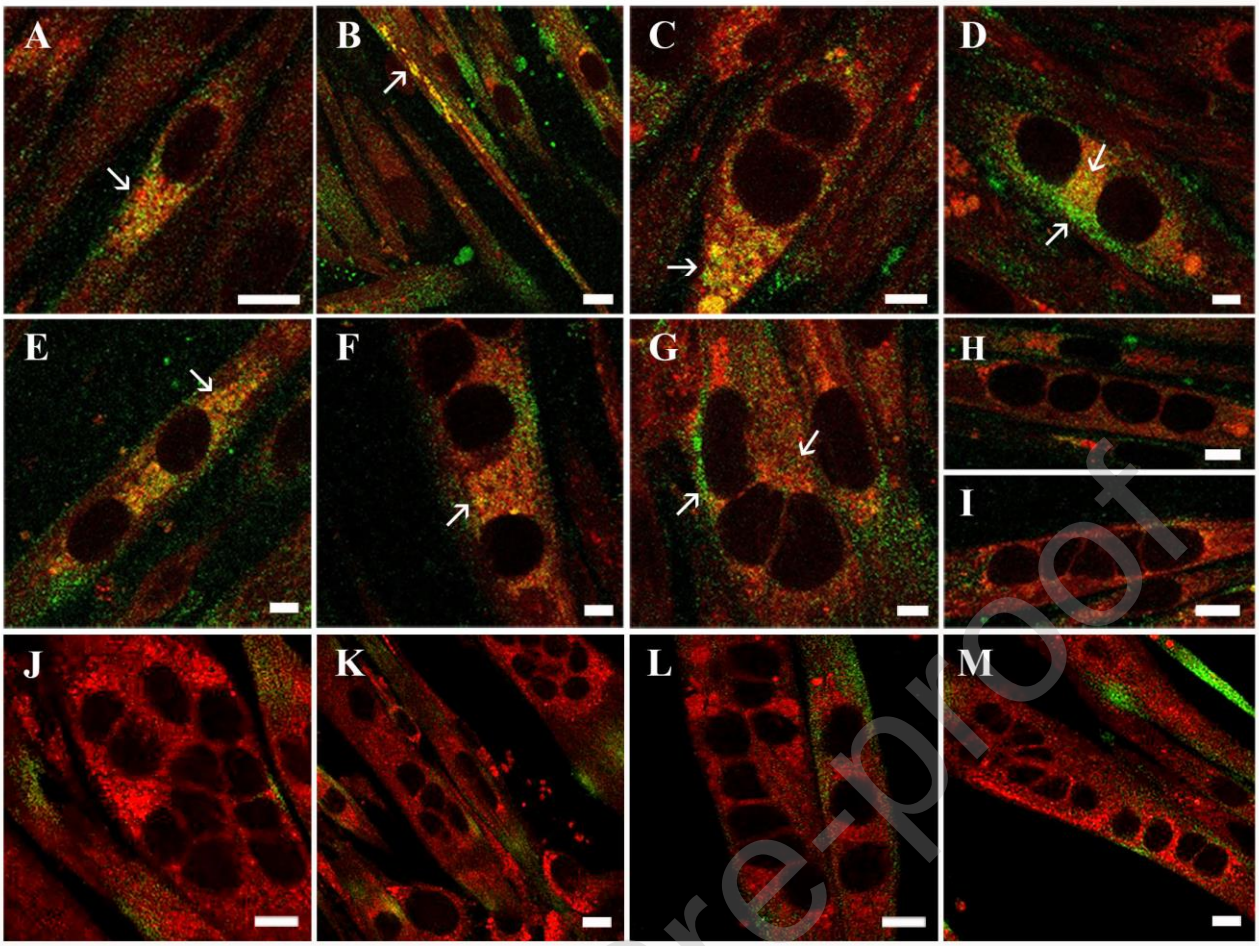

Figure 8. AA abolishes mitochondrial superoxide emission elicited by arsenite/ATP in C2C12 myoblasts, but not in myotubes.

Mb (A) and Mt (B) were initially pre-loaded (30 min) with MitoSOX red, subsequently exposed for 5 min to the vehicle, or 10 µM Ru360, and finally treated for a further 15 min with 10 µM arsenite, with or w/o ATP (100 µM). Insets: Mb (A) and Mt (B) were treated as previously indicated except that MitoSox Red was replaced with Rhod 2-AM. After treatments, the cells were analysed for their respective fluorescence responses. Results represent the means ± SD calculated from at least three separate experiments. **P < 0.01, as compared to untreated cells; (**)P < 0.01, or cells treated with arsenite/ATP (one-way ANOVA followed by Dunnet's test). (C) Mb and Mt were exposed for 10 min with increasing concentrations of AA, then loaded with MitoSox red and finally treated for 15 min with arsenite/ATP. After treatments, the cells were analysed for MitoSOX-fluorescence. (D) Mb

and Mt were exposed for increasing time intervals to 60 µM AA, and loaded with MitoSox red prior to treatment with arsenite/ATP. After treatments, the cells were analysed for MitoSOX-fluorescence. Results represent the means ± SD calculated from at three separate experiments. *P < 0.05; **P < 0.01 as compared to cells treated with arsenite/ATP (two-way ANOVA followed by Bonferroni's test).

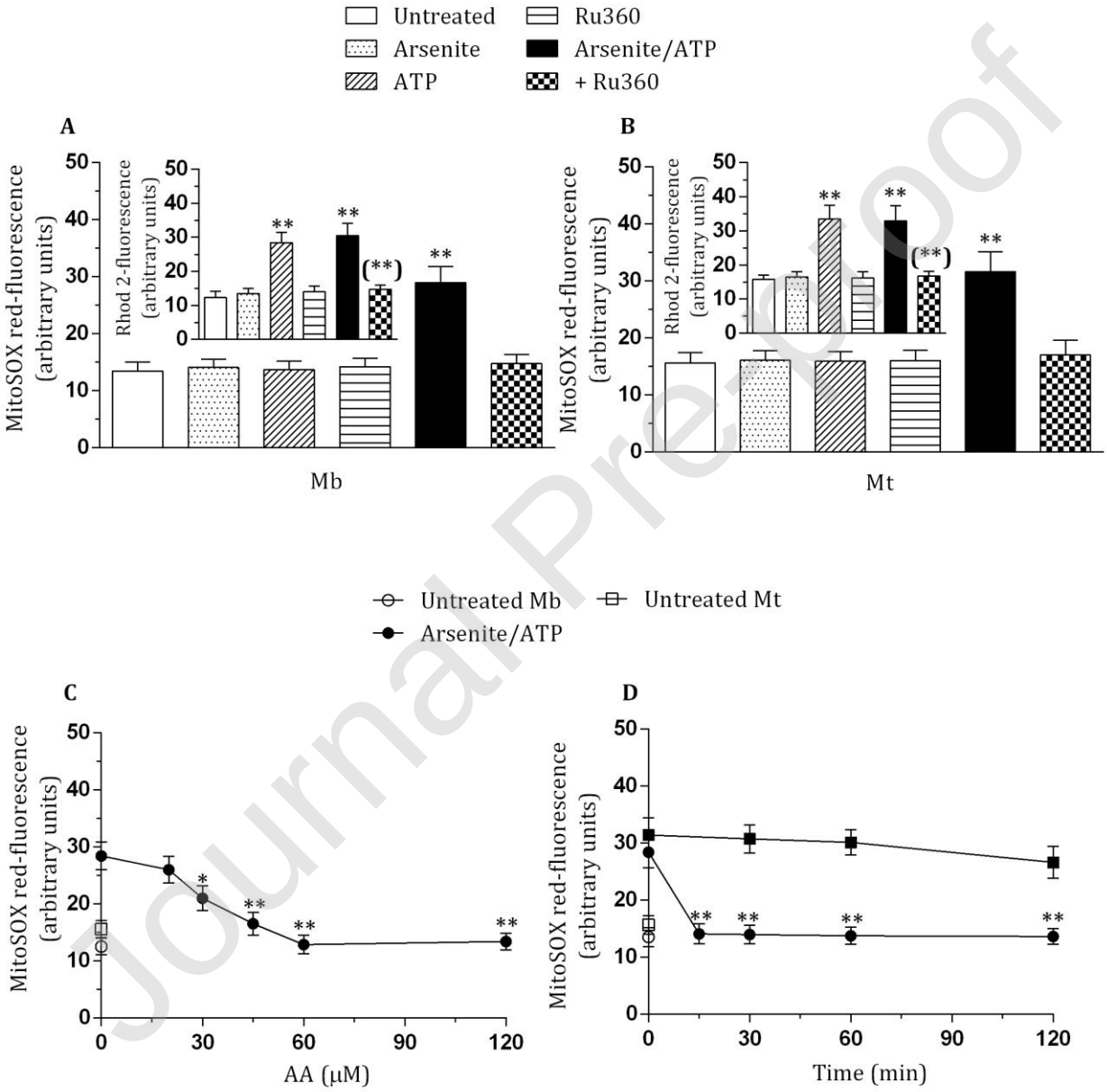

Figure 8

Figure 9. SVCT2 expression and transport of AA in Mb and early Mt plasma and mitochondrial membranes